Lipids (2013) 48:739–747
DOI 10.1007/s11745-013-3789-z

ORIGINAL ARTICLE

Fabrication of GM3-Enriched Sphingomyelin/Cholesterol Solid-Supported Lipid Membranes on Au/SiO_2 Plasmonic Substrates

G. Margheri · R. D'Agostino · M. Del Rosso · S. Trigari

Received: 3 October 2012 / Accepted: 26 March 2013 / Published online: 17 April 2013

Abstract The fabrication of solid-supported artificial lipid bilayers enriched with biological agents is an important step for acquiring more insights into their behavior from in vitro studies. In this work we demonstrate the formation of lipid artificial membranes enriched with ganglioside GM3, whose role in the cell proliferation and tumor angiogenesis is still an object of extensive investigation. The membranes are formed by fusion of small unilamellar vesicles (SUV) obtained from the sonication of multi-lamellar vesicles (MLV) formed from a hydrated mixture of GM3, brain sphingomyelin and cholesterol. The effective formation of SUV was confirmed by Dynamic light scattering (DLS) measurements. The recognition of the ganglioside in the biomimetic raft like biomembranes is accomplished via surface plasmon resonance (SPR) by exploiting the ganglioside affinity with wheat germ agglutinin (WGA). The affinity constant of the binding between the inglobated GM3 and WGA has been measured for three different GM3 molar concentrations. Beside the effective generation of GM3-enriched biomimetic membranes, our results indicate a decrease in the apparent WGA–GM3 dissociation constant at increasing GM3 concentrations up to 20 mol%, consistent with clustering effects of the ganglioside in the fabricated biomembranes.

Keywords Lipid rafts · Gangliosides · Surface plasmon resonance

Abbreviations

AFM	Atomic force microscope
DLS	Dynamic light scattering
WGA	Wheat germ agglutinin
SUV	Small unilamellar vesicle
MLV	Multi-lamellar vesicle
HBS	HEPES buffer solution
SPR	Surface plasmon resonance
PWR	Plasmon waveguide resonators
VEGF	Vascular endothelial growth factor
uPAR	Urokinase plasminogen activator receptor
ssBLM	Solid supported lipid bilayer membrane
SM	Brain sphingomyelin
POPC	1-Palmitoyl-2-oleoyl-*sn*-glycero-3-phosphocholine
Chol	Cholesterol
CTB	Beta subunit of the cholera toxin

Introduction

Systems mimicking the physiological cell membranes on solid supports (solid-supported bilayer lipid membranes, ssBLM) are excellent templates for studying their interactions in vitro with several biological molecules (ionic pumps, signalling agents, etc.…). Many of these molecules are recruited in particular mobile areas of the cell membrane, called lipid rafts [1], where microenvironmental effects on their functional properties can occur, with important pharmacological implications [2, 3].

G. Margheri (✉) · S. Trigari
Institute for Complex Systems, National Research Council, Via Madonna del Piano 10, 50019 Florence, Sesto Fiorentino, Italy
e-mail: giancarlo.margheri@isc.cnr.it

R. D'Agostino · M. Del Rosso
Department of Pathology and Experimental Oncology, University of Florence, Viale G.B.Morgagni 50, 50134 Florence, Italy

Among such molecules, the monosialodihexosylganglioside, GM3, whose abundance in lipid rafts has been documented by Simons and Ikonen [4], plays important roles in receptor functions and signal transduction [5], like for instance the suppression of the phosphorylation of the epidermal growth factor receptor [6, 7] and insulin receptor [8, 9] or the recognition of the influenza virus via its binding to the sialylgalactose structure of GM3 during the adsorption–fusion process [10]. Other experimental findings [11] indicate that the ganglioside GM3 blocks the cells proliferation induced by vascular endothelial growth factor (VEGF) and by the ganglioside GD1a, and it is also able to inhibit the linking between the urokinase plasminogen activator receptor (uPAR) and the integrin $\alpha_5\beta_1$ necessary for the migration of the endothelial cells [12]. Data on the ability of GM3 to inhibit the growth of tumor cells and tumor development as well as to increase symptom-free survival of mice grafted with human brain tumors are impressive [reviewed in 13]. Exogenous GM3 enrichment may suppress proliferation of many cancer cell lines [14–16], as well as inhibit mobility and angiogenesis of endothelial cells [13]. Overall, these effects must be referred to the supposed property of GM3 to inhibit macromolecular complexes of growth factor receptors, beta-integrins, kinases, and the transmembrane protein caveolin-1 acting as a scaffolding protein on aggregation of growth factor receptors.

Aiming to obtain an optimized replica of the ganglioside physiological behavior in vitro, its inglobation in artificial ssBLM biomembranes whose composition resembles that of physiological lipid rafts, namely a mixture of sphingomeylin (SM) and cholesterol (Chol), is a necessary prerequisite. Albeit its relevance, the recruitation of GM3 in biomimetic membranes and its binding properties to specific effectors is a scarcely present topic in the literature. The formation of GM3-enriched sphingomyelin-glucosylceramide mixed monolayers has been investigated with quartz crystal microbalance [17], while in another approach [18] the interaction of WGA with synthetic molecules possessing the same residual of *N*-acetylneuraminic acid of GM3 was studied by surface plasmon resonance (SPR). The generation of raft-like, GM3-rich domains in ssBLM made of phosphatidylcholine, sphingomyelin and cholesterol, has been accomplished by Iijima et al [19]. To our knowledge, this is so far the most exhaustive work on the self-organization of GM3 in bilayer lipid domains. Many aspects of the assembly of GM3 have been highlighted therein, for instance the fact that the organization of GM3 in the lipid rafts of living cells and in ssBLM composed of chemically defined lipids occurs in a similar way. These results were obtained thanks to the use of a sophisticated hardware for ssBLM fabrication and analysis, namely a Langmuir–Blodgett equipment and high resolution Atomic Force Microscope, whose resolution capability can be fully exploited only with the adoption of ultrasmooth mica substrates (external surface with $\sim$0.1 nm root-mean square roughness) as growth platforms for the biomembranes. However, important kinetic aspects related to the ganglioside organization in ssBLM could not be obtained, as for instance the variation of the ganglioside affinity for specific ligands with its concentration in the ssBLM.

In this work we report an alternative simple route to generate GM3-rich SM/Chol ssBLM onto silica-gold bilayers. The ssBLM enrichment with ganglioside, which is the fundamental task of our work, is monitored via SPR [20, 21] by exploiting the binding affinity between WGA and GM3 hosted in the SM/Chol ssBLM.

Our method of ssBLM formation is less refined than that described in [19], and the presence of GM3 in our binary ssBLM could not be monitored with a local analysis of the biomembranes, as the spectroscopic response is space-averaged on the laser spot size (diameter <1 mm). Nevertheless, the SPR spectroscopy has been effective in demonstrating the formation of ssBLM by liposomes fusion and in the recognition of GM3 in biomembrane matrix. Moreover, this technique allowed us to perform measurements of the WGA-GM3 affinity for different ganglioside loadings of ssBLM and to infer preliminary information on the ganglioside organization in these novel physiological-like structures.

Materials and Methods

The biomimetic membranes are formed by lipid vesicles fusion that occurs when liposomes are in contact with hydrophilic SiO_2 interfaces [22]. In order to guarantee the formation of more reproducible lipid bilayers, unilamellar vesicles are fabricated with a protocol similar to that described in [23]. First, stock solutions of GM3 and SM (both purchased from Santa Cruz Biotechnology, Santa Cruz, CA, and Avanti Polar, Alabaster, AL, respectively) were obtained by dissolving them at 2 mg/mL GM3 and 5 mg/mL SM in a mixture of $CHCl_3$/MeOH 4:1 by vol (both purchased from Sigma Aldrich, St. Louis, MO, USA), while Chol (Avanti Polar) was dissolved at 1 mg/mL in $CHCl_3$ to obtain the corresponding stock solution. The stock solutions were diluted and mixed to obtain four GM3 molar concentrations (0, 5, 10, 20 mol%). The different mixtures $GM3_x/SM_{0.6\text{-}x}/Chol_{0.4}$, where $x = 0$, 0.05, 0.1, 0.2 corresponds to 0, 5, 10, 20 mol% concentrations, were dried with a gentle flow of nitrogen and subsequently stored in a vacuum chamber overnight. After the solvent had completely evaporated, the lipid film was rehydrated with a total concentration of 1.6×10^{-7} mol/mL using HBS buffer solution (0.2 mg HEPES, pH 7.4, dissolved in

10 ml ultrapure water, 0.175 g NaCl dissolved in 10 mL ultrapure water. NaCl and HEPES were purchased from Sigma Aldrich, water was of Milli-Q purity, 18 MΩ cm resistivity) and vortexed for 30 min. An opalescent yellowish suspension of MLV was obtained, and this was sonicated at 60 °C for 30 min, to set an optically clear lipid suspension which consists of an emulsion of unilamellar vesicles. The distribution of their dimensions was measured with a dynamic light scattering (DLS) facility (Malvern Instruments Ltd). The vesicles emulsion obtained with each of the four GM3 concentrations was then injected into a PTFE cell that was hermetically sealed by the hydrophilic face of the optical transducer on which the vesicles fusion takes place.

The transducers are SF4 plano-parallel glass slides (Schott glass, refractive index = 1.74 at 633 nm) polished with a laser grade finish, covered with Au/SiO_2 films deposited with our high-vacuum e-gun-assisted evaporation facility, at a residual pressure of 5×10^{-6} Torr. Both Au and SiO_2 layers have equal nominal thicknesses of 50 nm (Au purity 99.95 % purchased from Goodfellow, Huntington, UK. SiO_2 powder, purity 99.95 %, purchased from Umicore, Bruxelles, B).The roughness of the transducer surface was measured with an Atomic Force Microscope equipment (Nanosurf Easyscan) on a sample area of 10×10 μm. Its root mean square (RMS) value, averaged from the 19 samples examined, was 0.4 nm, that is four times higher than that required for a high resolution AFM analysis ($\sim$ 0.1 nm).

The uncovered face of the transducer is coupled to the hypothenuse of a SF4 roof prism with an index matching oil (Cargille Labs. Cedar Grove, NJ, USA). The group formed by the prism-transducer-PTFE cell is hosted into the SPR spectrometer utilized for the optical characterizations of the fusion of the ssBLM and of the GM3-WGA binding reactions. The set-up and the SPR measurement approaches are shown in Fig. 1, while in Fig. 2, for the major suitability of the reader, we report the flow chart of a complete measurement run on the ssBLM:GM3.

The SPR spectrometer is a home-made instrument that exploits the classical Kretschmann scheme [24] in which the reflectance of a p-polarized collimated laser beam of a He–Ne laser (wavelength in vacuum: 633 nm) is measured vs the rotation angle of the optical transducer to obtain the SPR angular spectrum. This is characterized by the presence of a dip in the reflectivity at an incidence angle (resonance angle) that depends on the thickness and refractive index of the growing layer above the transducer. Alternatively, the reflectance is measured vs time at a fixed incidence angle to obtain the kinetic of the analyte-substrate binding reaction (sensorgram).

A first SPR spectrum is taken before the fusion process begins. Then the sensorgram of the fusion was recorded setting the spectrometer to an initial reflectivity of 0.3, that corresponds to the highest resolution of the configuration. As the process ends, typically after one hour, in order to check the stability of the membrane, a second SPR spectrum was recorded after three rinses.

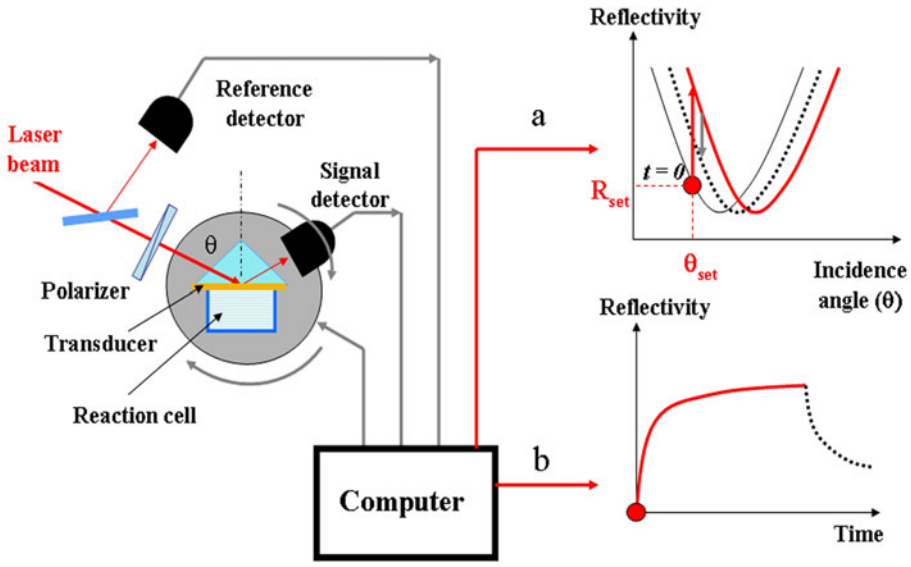

Fig. 1 Experimental layout and processing. A *p*-polarized laser beam impinges on the coupling prism, probes the plasmonic transducer, coupled to the reaction cell, and is reflected towards the signal detector. The reference and reflected signals are acquired by a PC, that drives the rotation of the prism and of the signal detector. When the refractive index of the solution-transducer interface changes in response to adsorption phenomena, the SPR spectrum recorded at $t = 0$ right shifts to the spectrum (*continuous lines*), that left shifts (*dashed line*) when detaching phenomena occur. Correspondingly, the sensorgrams (*b*) have an exponential increase (*continuous line*) or decrease (*dashed line*), respectively

After the completion of vesicles fusion, the association between GM3-enriched ssBLM and WGA was tested. This was accomplished injecting WGA (purchased from Sigma Aldrich)/HBS solutions at different WGA concentrations (1.25 , 2.5, 5, 10, 20 μM) into the PTFE cell, and recording the sensorgrams for each concentration. Besides the formation of WGA-GM3 complexes, weak aspecific accumulation of WGA on ssBLM may *a priori* occur, and must be removed. Following usual procedures, we rinsed the ssBLM with pure HBS three times, which would produce a fast detachment of weakly bound ligands. Subsequently, we filled the reaction cell with fresh buffer solution and let the system stabilize in consequence of the partial detachment of the WGA specifically bound to GM3, necessary to re-equilibrate the concentration of bound WGA with the buffer, that is WGA-free after rinsing. Both the rinsing and stabilization phases are continuously monitored by recording the sensorgrams in real time. So doing, slow or sudden reflectivity drops can easily identify the dissociation of specifically or aspecifically bound WGA respectively.

Further verifications of the specificity of WGA-GM3 binding were performed with two different approaches. First, we used ssBLM without GM3, obtained from the fusion of GM3-free SUV. After the completion of the fusion process, GM3-free ssBLM were put in contact with a 5 μM WGA/HBS solution and the corresponding control sensorgrams were recorded. Finally, we performed negative controls, putting in contact ssBLM:GM3 with a 5 μM solution in HBS of the beta-subunit of the Cholera toxin (CTB) (Sigma Aldrich, St. Louis, MO).

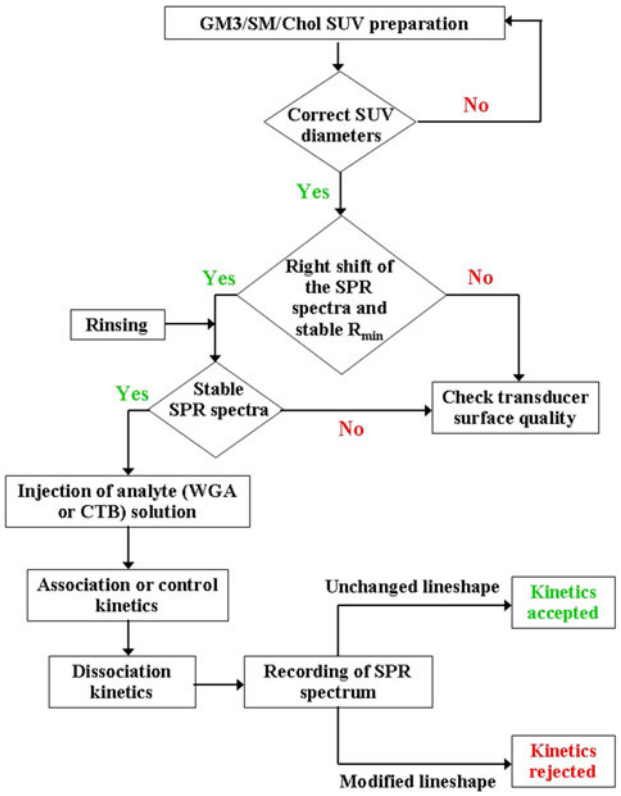

Fig. 2 Flow chart of the SPR measurement process

Results

The statistics of the vesicles radii obtained after the sonication of the MLV emulsions produced are reported in Fig. 3, where continuous, dashed and dotted curves correspond respectively to three GM3 concentrations, [GM3] = 20, 10 , 5 mol%. Two more samples emulsions were tested with [GM3] = 20 and 10 mol% concentrations to check the reproducibility of the vesicles dimensions. Such tests are reported in the same figure with two further continuous and dashed curves respectively. These statistics are unimodal, with average radius (45 ± 15) nm, indicating the effective formation of small unilamellar vesicles (SUV). The curves of Fig. 3 show that the radii distributions are almost independent from the lipids concentrations used.

Curve (a) in Fig. 4 reports an example of the SPR spectra of a solution of vesicles constituted of a $GM3_{0.1}$/$SM_{0.5}$/$Chol_{0.4}$ mixture, while curve (b) shows the spectrum taken after their fusion on SiO_2 and three rinsing cycles, performed to check the stability of the assembled membrane. Both spectra have the same minimum reflectivity $R_{min} = 0.02$, while the resonance angle is 1.3° apart. Similar results were obtained for ssBLM obtained for [GM3] = 20 and 5 mol%.

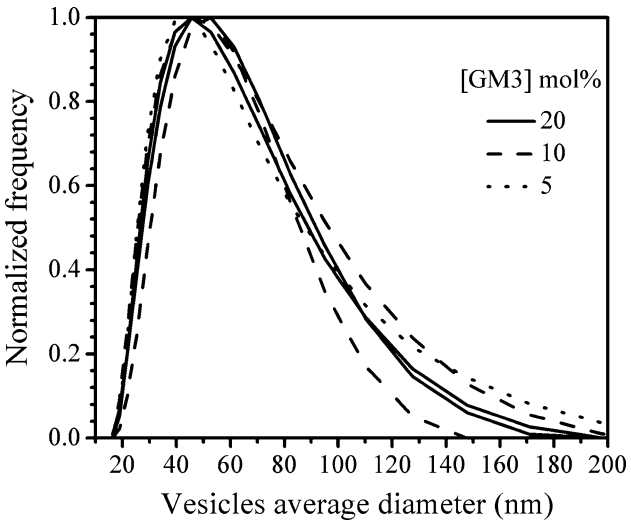

Fig. 3 DLS statistics of the radii of the GM3/SM/Chol unilamellar vesicles after the sonication. *Continuous lines* are relative to [GM3] = 20 mol%, *dashed lines* are relative to [GM3] = 10 mol% and *dotted line* to [GM3] = 5 mol%

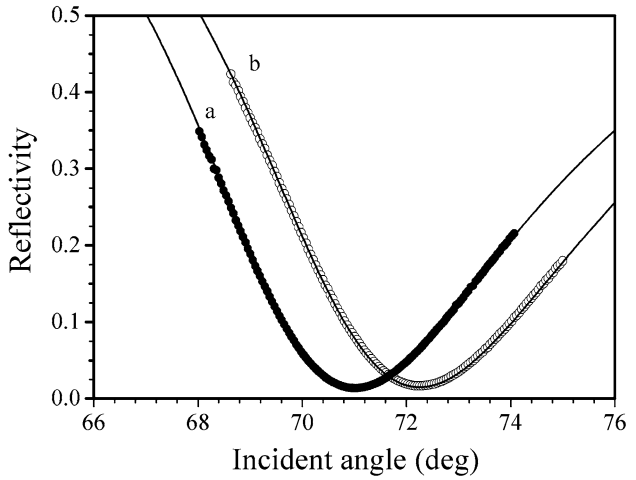

Fig. 4 SPR spectra obtained before (*a*) and after (*b*) the fusion of SUV with $GM3_{0.1}/SM_{0.5}/Chol_{0.4}$. The Au and SiO_2 thicknesses calculated by the best fit of the spectra (*continuos lines*) are 48.9 nm for Au and 44.2 nm for SiO_2, while the dielectric constants are $-11.74 + 1.47i$ (Au) and 2.10 (SiO_2). The HBS buffer solution has a dielectric constant of 1.769

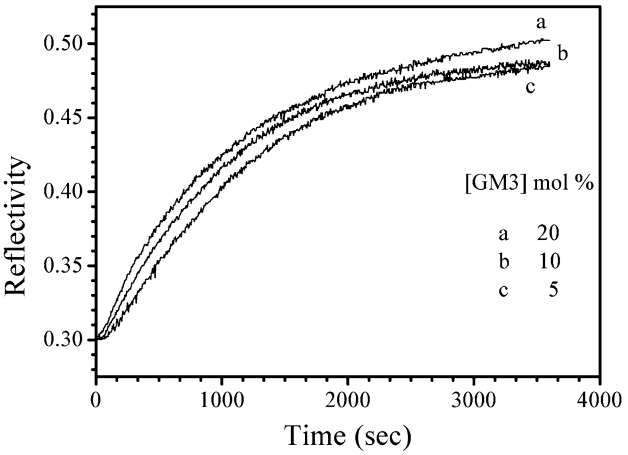

Fig. 5 Kinetics of the fusion on Au-SiO_2 films of SUVs with [GM3] (from up to down) 20 mol% (**a**), 10 mol% (**b**), 5 mol% (**c**) in the GM3/SM/Chol lipid mixture

Considering the dielectric constant of SiO_2 the value to be 2.10, the best fitting of the spectrum (a) (continuous line), allowed us to complete the characterization of the transducing multilayer. The best fit was performed with the open source software WINSPALL, freely available on the Internet, which can be used both to compute the reflectivity of a plane wave when it impinges on a multilayer with plano-parallel interfaces or, as in our case, to determine the optical parameters of a planar stratification from the best fit of the measured SPR angular spectrum. The values found for the dielectric constant of Au was $-11.74 + 1.47i$. The thicknesses are 48.9 nm for gold and 44.2 nm for SiO_2, in good agreement with the nominal ones.

The fusion of liposomes on SiO_2 layer for the three considered mixtures is monitored in real time, producing the sensorgrams reported in Fig. 5.

The reflectivity variations are 0.2 for the formation of membranes with $x = 0.2$ and 0.17 for membranes with $x = 0.05$ and 0.1, thus the smoothness of the self-assembled membranes is similar. Our SPR measurement method allowed us to study the association-dissociation kinetics of WGA with the ssBLM. For each WGA concentration we used a different ssBLM:GM3, with an overall number of 19 ssBLM examined.

The kinetics of WGA-GM3 binding deserves particular attention, since, to our knowledge, it has not been previously studied in a physiological-like ganglioside host. The sensorgrams are characterized by a fast initial association kinetic described by the exponential model [25]

$$\Delta R_{\mathrm{ass}}(t) = \Delta R_0(1 - \mathrm{e}^{-k_{\mathrm{on}}t}) \quad (1)$$

where $\Delta R_{\mathrm{ass}}(t)$ is the reflectivity change vs time, ΔR_0 is the regime value of the fast part of the kinetic and k_{on} is its time constant, evaluated by best fitting the experimental sensorgrams. k_{on} depends on the concentration of the free WGA via the ligand-receptor dissociation-association constants, k_{diss} and k_{ass}, respectively. This dependence is described by the linear relationship [25]

$$k_{\mathrm{on}} = k_{\mathrm{diss}} + k_{\mathrm{ass}}[\mathrm{WGA}] \quad (2)$$

where [WGA] is the WGA molar concentration in HBS and k_{diss} is the dissociation constant of the complex GM3-WGA. When the substrate is substituted by HBS alone, the WGA-GM3 dissociation occurs, following an exponential kinetic

$$\Delta R_{\mathrm{diss}}(t) = (\Delta R_{\mathrm{fin}} + \Delta R_1 \cdot \mathrm{e}^{-k_{\mathrm{diss}}t}) \quad (3)$$

where $\Delta R_{\mathrm{diss}}(t)$ is the the reflectivity change vs time, ΔR_{fin} is its equilibrium value at the end of the dissociation phase and ΔR_1 is the reflectivity difference between the ends of the association and dissociation phases.

The quantities R_{fin}, $\Delta R_{0,1}$ defined in Eqs.1, 3 depend on the equilibrium between the concentration of WGA bound on the ssBLM:GM3 and the free WGA in the buffer solution. For instance, in the presence of a continuous flow during the rinsing phases, there is a continuous detachment of WGA from the ssBLM, so that the overall reflectivity variation with respect to the initial setpoint (0.3) is $\Delta R_{\mathrm{fin}} = 0$. On the contrary, in our case, the rinsing stops after some time. As a consequence, a new equilibrium is reached with $\Delta R_{\mathrm{fin}} \neq 0$.

Direct evaluation of both k_{ass} and k_{diss} can in principle be performed by best fitting of the k_{on}-[WGA] data with the

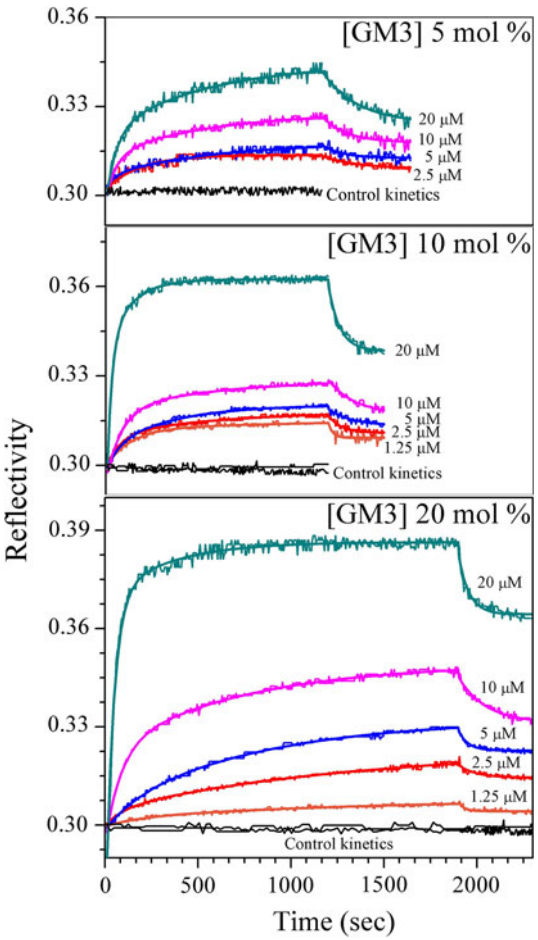

Fig. 6 Association and control kinetics during the incubation of WGA-HBS solutions at various WGA concentrations in contact with SM/Chol ssBLM:GM3 obtained from the fusion of vesicles at the three different GM3 loadings 5, 10, 20 mol%. The best fits (*continuous lines*) have been superimposed to the experimental traces

model described by Eq. 2, but the value of k_{diss} is often close to zero and inaccurately defined [25]. Hence, we have measured k_{diss} better by removing the free ligand and directly monitoring the WGA-GM3 dissociation after the HBS has been injected in the reaction cell. By best fitting the sensorgrams of the dissociation phases, the value of k_{diss} was calculated for each dissociation kinetic. The association-dissociation kinetics and the control kinetics (these last recorded with GM3-free ssBLM), have been embedded with their best-fit in Fig. 6, whose subsections refer to [GM3] = 20 mol%, [GM3] = 10 mol% and [GM3] = 5 mol%, respectively.

The average value of k_{diss}, $k_{dissav,}$ was considered as the dissociation constant of WGA-GM3 complex for the corresponding GM3 concentration in the initial mixture. The plots of k_{on} versus [WGA] for each GM3 concentration (Fig. 7), confirmed the linear trends predicted by Eq. 2. Their best fitting allowed to calculate k_{ass} for each GM3 concentration.

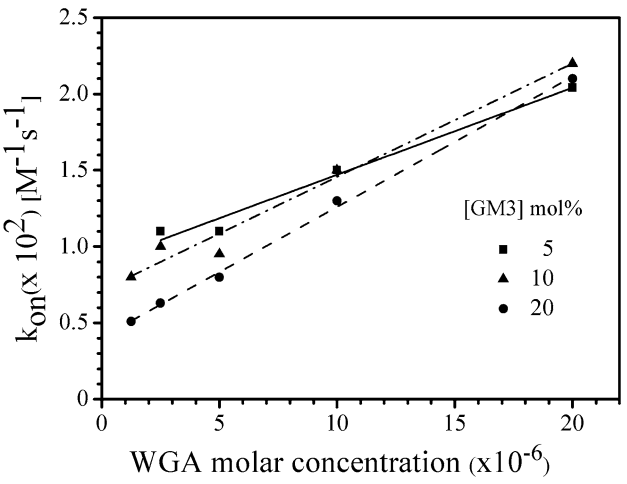

Fig. 7 Experimental association rate constants k_{on} and their best-fits (modeled with Eq. (2)) vs WGA molar concentration. The GM3 molar concentration in the initial lipid mixture are: 5 mol% (*filled square*, best fitting: *continuous line*), 10 mol% (*filled triangles*, best fitting: *dotted line*), 20 mol% (*filled circles*, best fitting: *dashed line*)

Finally, the value of the apparent dissociation constant K_D, whose inverse K_D^{-1} defines the apparent binding affinity constant, is calculated as

$$K_D = \frac{k_{dissav}}{k_{ass}} \quad (4)$$

The values of K_D, k_{ass}, k_{dissav} are summarized in Table 1 along with the GM3 concentration.

Discussion

The main task of our work was to demonstrate the fabrication of homogeneous and stable SM/Chol ssBLM:GM3. Indeed, homogeneity and stability are of most concern in the fabrication of ssBLM biomimetic structures.

Provided that the growth support has a small enough roughness, the formation of ssBLM via liposomes fusion onto a hydrophilic surface is a well-assessed route to fabricate homogeneous ssBLM. In our case, the average RMS roughness of the supports was 0.4 nm, that is of the same order of magnitude of that exhibited by the ultrasmooth supports used to perform similar investigations with AFM

Table 1 Kinetic constants of the binding process between WGA and the GM3 inglobated in the artificial SM/Chol ssBLM for different GM3 concentrations

[GM3] (mol%)	k_{ass} (M^{-1} s^{-1})	k_{dissav} (s^{-1})	K_D (μM)
5	$(5.7 \pm 0.6) \times 10^2$	0.009 ± 0.0006	16.0 ± 1.6
10	$(7.2 \pm 1.4) \times 10^2$	0.0069 ± 0.0005	10 ± 0.7
20	$(8.5 \pm 2.5) \times 10^2$	0.004 ± 0.0008	5.6 ± 1.3

equipment [19]. So we expect trends in the SPR spectra consistent with the formation of homogeneous ssBLM. Indeed, the right shift of 1.3° of the SPR spectrum with the unchanged minimum reflectivity, reported in Fig. 4, is a confirmation that the liposomes fusion has correctly occurred [26]. Further checks were performed by recording the SPR spectra after rinses and after the addition of WGA. In both cases, these spectra (data not shown) remain stationary or have a left shift with unchanged minima. This spectral behavior is reflected in stationary or weakly decreasing control sensorgrams, indicating a weak instability of the biomembrane. However, rather than an influence of WGA on the membrane structure, the observed degradation is more likely due to the presence of a small amount of non fused or hemifused SUV, that interacts too weakly with SiO_2 and can easily detach from the surface [22]. Also, we have observed no significant change in the position of the critical angle [21] with pure buffer solution, with SUV solutions or by addition of WGA solutions, indicating that the interference of the bulk solution on the observed kinetics is negligible.

Finally, the constancy of the minimum reflectivity and the lack of deformation of the SPR spectra during the recognition process indicate the correctness of the kinetics recording procedure at a constant interrogation angle. This method is alternative to the widely used one consisting in recording the shifts of the angular positions of the reflectivity minima (namely the plasma angles) vs time [21, 27].

The presence of GM3 in the ssBLM was verified by two different measurements. First, we measured the refractive index difference between the ganglioside free- ssBLM and that of the GM3-rich ssBLM. Indeed, the recruitation or recognition events may lead to a significative variation of the ssBLM refractive index, that can thus be exploited as a tool to detect the incorporation of physiological agents. For instance, in [23] a decrease in the refractive index (−0.085) of a POPC ssBLM was found as a consequence of the recruitation of the protein β-amyloid in the ssBLM, and was attributed to the partial loss of lipid packing due to the amyloid-membrane interaction. Similar rearrangement phenomena can also lead to mechanical-optical anisotropic rearrangements of ssBLM, producing different refractive index changes for *s* and *p* polarizations, even of opposite signs, monitorable with another plasmonic tool, namely the Plasmon Waveguide Resonator (PWR) technique [28].

In our case, we calculated the refractive index of the ssBLM by best fitting the SPR spectrum after the liposomes fusion has occurred. Supposing that the membrane has a thickness of 5.5 nm, namely the same value reported for similar ones enriched with the ganglioside GM1 [22], the best fit gives a refractive index of 1.525, lower than that (1.555) found for membranes formed from GM3-free lipids mixtures. This decrease is analogous to the observation reported in [23], so we assume that also in our case a loss in lipids packing has been induced on $SM_{0.6}/Chol_{0.4}$ membranes by the presence of GM3.

Albeit the recruitation processes can thus be monitored via the induced refractive index changes, affordable measurements require the precise evaluation in situ of the thickness and refractive index of the biomembrane before its local modification occurs, a complex task to get by the SPR technique. Thus, our preliminary indication of the effective GM3 presence has been more directly verified with successive experiments where SPR monitored the WGA-GM3 binding.

As SPR is a label-free technique, it is necessary to ensure that aspecific interactions between the analyte and the adsorbing host have negligible effects. The specificity was tested both with control kinetics using GM3-free ssBLM and with negative controls on GM3-enriched ssBLM, by recording the kinetics in the presence of a 5 μM amount in HBS solution of the beta-subunit of the cholera toxin (CTB), that has been demonstrated to exhibit no detectable affinity with GM3 recruited in POPC ssBLM [29].

The lack of interaction of WGA with GM3-free ssBLM is demonstrated by the substantial stability of the control traces reported in Fig. 6. A similar trend was found in the negative tests performed with CTB, in agreement with the results of [29]. Another check on the aspecific binding of WGA due to its weak accumulation on the SM/Chol ssBLM:GM3 was performed by recording the sensorgrams after the rinses following the association phases. Actually, the sensorgrams did not suffer significant changes, indicating that aspecific weak binding of WGA was not the main concern. The sensorgrams of Fig. 6 definitely demonstrate the specific recognition of GM3, and as a consequence the successful achievement of our goal, namely the generation of SM/Chol ssBLM:GM3.

Even if the GM3 presence is the necessary prerequisite to exploit these ssBLM fruitfully, many of the GM3-dependent biological effects are still waiting for a mechanistic explanation based on the role that the ganglioside enrichment plays in affecting its properties throughout its organization in the lipid matrix, like for example, the affinity with critical lipid-raft-associated molecules, or also with other non-rafts ligands like WGA. In this last case, the variation of the affinity of GM3 hosted in SM/Chol ssBLM may thus be exploited as a tool to obtain information on the organization of the ganglioside in the physiological lipid-raft domains. Aiming to obtain preliminary indications in this direction, we carried out measurements on the WGA-GM3 affinity using ssBLM:GM3 at various GM3 enrichments. A decreasing trend of the apparent dissociation constant k_{dissav} was found (Table. 1), passing from (16.0 ± 1.6) μM at [GM3] = 5 mol% to (5.6 ± 1.3) μM

at [GM3] = 20 mol%, while the dissociation constants k_{diss} decreases with enrichment. A similar effect has been previously observed, like for instance in the case of the binding between chymotrypsin and recombinant chymotrypsin inhibitor CI-2 [25].

As anticipated, to our knowledge these are the first results on the binding between WGA and GM3 hosted in a binary ssBLM environment resembling the composition of lipid rafts, so only a rough comparison with other GM3-hosting biomembranes can be made. In [18] the affinity of WGA for a synthetic molecule, the *N*-acetyl-D-glucosamine (GlcNAc), possessing the same residual of *N*-acetylneuraminic acid of GM3, was measured with SPR. In this case, the apparent dissociation constant spanned from 44 to 165 μM depending on the concentration of GlcNAc (100 nM to 5 mM). Although the large difference between our membrane model (that is a bilayer membrane) and the tests reported in [18], where WGA was immobilized on a BIAcore sensing chip instead of GM3 (that had the role of analyte), K_D of the same order of magnitude were found, showing a similar extent of WGA-GM3 binding strength.

A system more similar to our ssBLM has been considered in [17], where the binding of WGA to GM3 loaded on a non-immobilized sphingomyelin monolayer in a (5/95) mol% composition was studied. The apparent dissociation constant, as computable from the reported data, results in $K_D = 12.5$ μM, which is in good agreement with that found by us for the same composition. Findings of [17] also indicate another similarity, that is, the increasing trend in the WGA-GM3 binding strength with [GM3]. Indeed, both binding rates and the maximum bound mass of WGA increase until [GM3] = 20 mol%, that is the concentration maximizing their values. These observations are consistent with the modulation of the recognition process of gangliosides in lipid membranes induced by cluster effects, whose occurrence was established quite some time ago [30].

Depending on the ganglioside structure and hosting matrix, clustering can produce either an increase, as in our case, or a decrease (negative clustering effect) of the apparent affinity for a given ligand, as in the relevant case of the binding of ganglioside GM1 with CTB [17, 31, 32]. For instance, the increase of the apparent affinity with [GM3] in phospholipid matrices was explained in [17] with the fact that when GM3 is present in amounts much lower than 20 mol%, the ganglioside-lipid matrix interaction partially hides the anchoring sites and prevents WGA binding, resulting in its lower avidity. As [GM3] increases, the ganglioside tends to form clusters that prevent its interaction with the lipids matrix, setting free more anchoring sites for binding to GM3, that in this way can optimally exploit the four binding sites of WGA for sialic acid [33].

In conclusion, we have reported on the generation of stable SM/Chol ssBLM hosting the ganglioside GM3 on a plasmonic support. The effective presence of this ganglioside in the biomembranes was detected by SPR measurements, by exploiting the affinity of GM3 with WGA. This method also allowed us to measure the apparent dissociation constant of WGA-GM3 complexes for three different GM3 enrichments. It exhibits a decrease with GM3 concentration in ssBLM, suggesting the occurrence of clustering effects of GM3 in the artificial biomembrane at increasing ganglioside concentrations. However, the assessment of definitive conclusions on the GM3 organization in our SM/Chol artificial biomembranes would require more dedicated investigations to better clarify the factors that influence the binding of the hosted GM3 to WGA, as for example the cholesterol abundance, that modulates the lipids packing in the lipid raft domains, and pH, that is 7.4 ± 0.1 in the extracellular environment (thus very close to that adopted by us), but is around 6.8 inside the cell.

The simple diagnostic method based on SPR gives only space-averaged information on the GM3 presence in the ssBLM, but was anyhow effective to demonstrate the validity of the proposed route to fabricate ganglioside enriched ssBLM, to monitor the quality of the biomembranes, and to detect a receptor enrichment. The method seems to be particularly simple and suitable both to evaluate the apparent dissociation constant of GM3 as well as of other recruitable receptors, and to infer information on their reorganization ways in the ssBLM, that modulate the recognition process of ligands. How such receptors and the complexes that they can form are organized within lipid-rafts is still a matter of scientific debate. The possibility to fabricate easily GM3-enriched solid-supported binary ssBLM resembling the composition of physiological lipid rafts, as described in this work, may offer a new tool to provide a scientific basis to the biological observations.

Acknowledgments The authors wish to thank Drs. Fabrizio Pieralli for his support in the fabrication of SPR transducers, Davide Scarpellini and Paolo Paoli for their contribution in the fabrication and characterization of vesicles emulsions. This work has been supported by the project "Coinvolgimento di lipid rafts in medicina molecolare" funded by Ente Cassa di Risparmio di Firenze (ECRF), grant n°2010.0622.

References

1. Hooper NM (1998) Membrane biology: do glycolipid microdomains really exist? Curr Biol 8:114–116
2. Chini B, Parenti M (2004) G-protein coupled receptors in lipid rafts and caveolae: how, when and why do they go there? J Mol Endocrinol 32:325–338
3. Ostrom RS, Insel PA (2004) The evolving role of lipid rafts and caveolae in G protein-coupled receptor signaling: implications for molecular pharmacology. Br J Pharmacol 145:235–245
4. Simons K, Ikonen E (1997) Functional rafts in cell membranes. Nature 387:569–572

5. Hakomori S (2001) Membrane microdomains defining cell adhesion and signaling. Trends Glycosci Glycotechnol 13:219–230
6. Bremer EG, Schlessinger J, Hakomori S (1986) Ganglioside-mediated modulation of cell growth. J Biol Chem 261:2434–2440
7. Miljan EA, Meuillet EJ, Mania-Farnell B, George D, Yamamoto H, Simon HG, Bremer EG (2002) Interaction of the extracellular domain of the epidermal growth factor receptor with gangliosides. J Biol Chem 277:10108–10113
8. Nojiri H, Stroud M, Hakomori S (1991) A specific type of ganglioside as a modulator of insulin dependent cell growth and insulin receptor tyrosine kinase activity. Possible association of ganglioside-induced inhibition of insulin receptor function and monocytic differentiation induction in HL-60 cells. J Biol Chem 266:4531–4537
9. Kabayama K, Sato T, Kitamura F, Uemura S, Kang BW, Igarashi Y, Inokuchi J (2005) TNFα-induced insulin resistance in adipocytes as a membrane microdomain disorder: involvement of ganglioside GM3. Glycobiology 15:21–29
10. Suzuki Y (1994) Gangliosides as influenza virus receptors. Variation of influenza viruses and their recognition of the receptor sialo-sugar chains. Prog Lipid Res 33:429–457
11. Alessandri G, Cornaglia-Ferraris P, Gullino PM (1997) Angiogenic and angiostatic microenvironment in tumors: role of gangliosides. Acta Oncol 36:383–387
12. Mukherjee P, Faber AC, Shelton LM, Baek RC, Chiles TC, Seyfried TN (2008) Thematic review series: sphingolipids. Ganglioside GM3 suppresses the proangiogenic effects of vascular endothelial growth factor and ganglioside GD1a. J Lipid Res 49:929–938
13. Brokazova NV, Samovilova NN, Gracheva EV, Golovanova NK (2009) Ganglioside GM3 and its biological functions. Biochemistry (Moskow) 74:293–308
14. Rebbaa A, Hurh J, Yamamoto H, Kersey DS, Bremer EG (1996) Ganglioside GM3 inhibition of EGF receptor mediated signal transduction. Glycobiology 6:399–406
15. Noll EN, Lin J, Nakatsuji Y, Miller RH, Black PM (2001) GM3 as a novel growth regulator for human gliomas. Exp Neurol 168:300–309
16. Fujimoto Y, Izumoto S, Suzuki T, Kinoshita M, Kagawa N, Wada K, Hashimoto N, Maruno M, Nakatsuji Y, Yoshimine T (2005) Ganglioside GM3 inhibits proliferation and invasion of glioma. J Neurooncol 71:99–106
17. Sato T, Serizawa T, Ohtake F, Nakamura M, Terabayashi T, Kawanishi Y, Okahata Y (1998) Quantitative measurements of the interaction between monosialoganglioside monolayers and wheat germ agglutinin (WGA) by a quartz-crystal microbalance. Biochim Biophys Acta 1380:82–92
18. Lienemann M, Paananen A, Boer H, De la Fuente JM, Garcia I, Penades S, Koivula A (2009) Characterization of the wheat germ agglutinin binding to self-assembled monolayers of neoglycoconjugates by AFM and SPR. Glycobiology 19:633–643
19. Iijima K, Soga N, Matsubara T, Sato T (2009) Observations of the distribution of GM3 in membrane microdomains by atomic force microscopy. J Colloid Interf Sci 337:369–374
20. Homola J (2008) Surface plasmon resonance sensors for detection of chemical and biological species. Chem Rev 108:462–493
21. Piliarick M, Homola J (2009) Surface plasmon resonance sensors: approaching their limits? Opt Express 17:16505–16517
22. Mao Y, Tero R, Imai Y, Hoshino T, Urisu T (2008) The morphology of $GM1_x/SM_{0.6-x}/Chol_{0.4}$ planar bilayers supported on SiO_2 surfaces. Chem Phys Lett 460:289–294
23. Devanathan S, Salamon Z, Lindblom G, Grobner G, Tollin G (2006) Effects of sphingomyelin, cholesterol and zinc ions on the binding, insertion and aggregation of the amyloid A1-40 peptide in solid-supported lipid bilayers. FEBS J 273:1389–1402
24. Raether H (1981) Surface plasmons on smooth and rough surfaces and on gratings. Springer-Verlag, Berlin
25. Edwards PR, Lowe PA, Leatherbarrow RJ (1997) Ligand loading at the surface of an optical biosensor and its effect upon the kinetics of protein–protein interactions. J Mol Recognit 10:128–134
26. Fontana E, Pantell RH (1988) Characterization of multilayer rough surfaces using surface plasmon spectroscopy. Phys Rev B 37:3164–3182
27. Horn N, Kreiter M (2010) Plasmon spectroscopy: methods, pitfalls and how to avoid them. Plasmonics 5:331–345
28. Hruby VJ, Alves I, Cowell S, Salamon Z, Tollin G (2010) Use of plasmon waveguide resonance (PWR) spectroscopy for examining binding, signalling and lipid domain partitioning of membrane proteins. Life Sci 86:569–574
29. Janshoff A, Steinem C, Sieber M, El Baya A, Schmidt MA, Galla HJ (1997) Quartz crystal microbalance investigation of the interaction of bacterial toxins with ganglioside containing solid supported membranes. Eur Biophys J 26:261–270
30. Delmelle M, Dufrane SP, Brasseur R (1980) Clustering of gangliosides in phospholipids bilayers. FEBS Lett 121:11–14
31. Shi J, Yang T, Kataoka S, Zhang Y, Diaz AJ, Cremer PS (2007) GM1 clustering inhibits cholera toxin binding in supported phospholipid membranes. J Am Chem Soc 129:5954–5961
32. Margheri G, D'Agostino R, Becucci L, Guidelli R, Tiribilli B, Del Rosso M (2012) Surface plasmon resonance as detection tool for lipids lateral mobility in biomimetic membranes. Biomed Opt Express 3:3119–3126
33. Bhayanandan VP, Katlic AW (1979) The interaction of wheat germ agglutinin with sialoglycoproteins. The role of sialic acid. J Biol Chem 254:4000–4008